ROYAL SOCIETY OF CHEMISTRY

PERSPECTIVE

I+/I2/I− conversion toward energy-dense aqueous Zn–I2 batteries: progress and perspective

Yangyang Liu, Kuan Zhou, Rui Wang, Quanwei Ma, Peng Xiong, Longhai Zhang* and Chaofeng Zhang [ID] *

Aqueous zinc–iodine batteries (ZIBs), exploiting reversible conversion among various iodine species, have drawn significant research interest due to their fast redox kinetics and capability for multi-electron transfer. Although significant progress has been made in ZIBs based on the two-electron I_2/I^- redox pathway (2eZIBs), their inherently limited energy density impedes practical deployment. Achieving the additional reversible conversion of high-valence iodine species, particularly the I^+/I_2 redox chemistry, offers substantial potential for improving energy density up to 630 Wh kg^{-1} based on the mass of I_2. Nonetheless, Zn–I2 batteries based on this four-electron $I^+/I_2/I^-$ conversion (4eZIBs) suffer from severe reversibility issues due to the shuttle of iodide intermediates and the detrimental hydrolysis of I^+ species during the conversion process. In this perspective, we comprehensively elucidate the fundamental principles of the I_2/I^- and I^+/I_2 redox chemistry, while critically evaluating the merits and limitations of diverse strategies for enhancing the performance of 4eZIBs. Significantly, we propose specific methodological approaches from multiple angles to improve the reversibility of $I^+/I_2/I^-$ conversion. These findings aim to provide valuable insights for the development of advanced metal–halogen battery energy storage systems.

1. Introduction

The energy crisis and emerging climate change caused by CO_2 emissions have driven the search for green and sustainable energy sources such as solar, wind, and so on.[1] Because of the

School of Materials Science and Engineering, Institutes of Physical Science and Information Technology, Leibniz International Joint Research Center of Materials Sciences of Anhui Province, Anhui University, Hefei 230601, China. E-mail: zlhedu@ahu.edu.cn; cfz@ahu.edu.cn

intermittence of these renewable energy sources, energy storage technologies such as batteries are needed to integrate them into the grid.[2,3] Since their commercialization in 1991, lithium-ion batteries (LIBs) have dominated energy storage and conversion systems in portable electronic devices, electric vehicles, and smart grids. However, the high cost and safety risks limit their application in large-scale energy storage devices.[4,5] Aqueous rechargeable Zn batteries (AZBs) present a promising solution for large-scale energy storage owing to their high safety, high capacity of Zn (820 mAh g^{-1} or 5855 mAh cm^{-3}), low

Dr Yangyang Liu is now a post-doctoral researcher at Anhui University, Hefei, China. He received his PhD degree from the Shanghai Institute of Ceramics, Chinese Academy of Sciences in 2022, after graduating from Tongji University with an MSc in 2019. His current research interests focus on the design of advanced electrolytes for aqueous Zn-based batteries and the investigation of electrode/electrolyte interfaces.

Yangyang Liu

Dr Longhai Zhang is currently a lecturer at the Institutes of Physical Science and Information Technology, Anhui University, Hefei, China. He received his BSc and MSc degrees from Anhui University of Technology. Then, he obtained his PhD degree in 2019 from Harbin Engineering University. His research focuses on the synthesis of organic electrode materials for energy storage (Li/Na-ion batteries and aqueous Zn/Al-ion batteries).
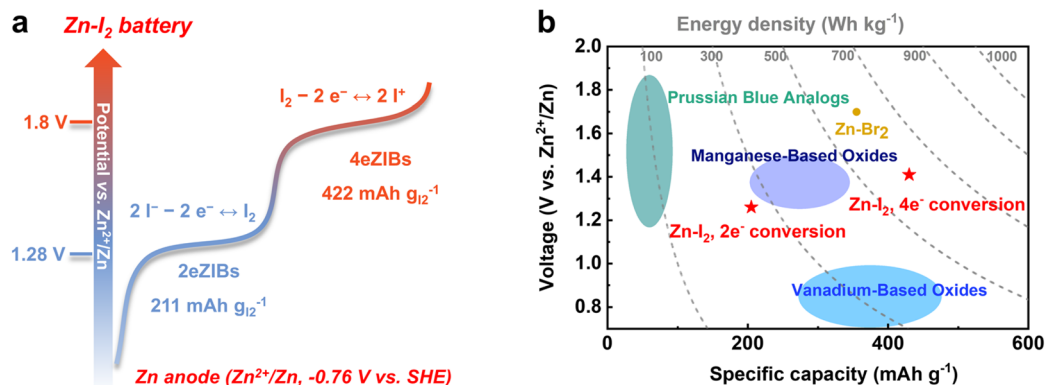
Longhai Zhang

Fig. 1 Comparison of energy density of ZIBs with exiting AZBs. (a) Schematic for iodine conversion. (b) Theoretical energy density of commonly used cathodes for AZBs.

cost, and eco-friendliness.[6–9] Therefore, developing AZBs is crucial for advancing large-scale energy storage technologies.

Rechargeable aqueous Zn–halogen batteries employing typical conversion-type cathodes ($I_2/Br_2/Cl_2$) have garnered significant attention, benefiting from their stable redox reactions and fast conversion kinetics associated with the Zn^{2+}/H^+-independent mechanism.[10–14] Additionally, the multielectron conversion process significantly enhances their capacity and energy density. Specifically, I_2 cathodes are particularly promising due to their low solubility in water (≈ 0.29 g L^{-1}), moderate operating potential, and abundance in oceanic reserves, making them suitable for stationary aqueous Zn–I_2 batteries (ZIBs).[15,16] As shown in Fig. 1a, the I_2 cathode delivers a theoretical capacity of 211 mAh g^{-1} based on a typical two-electron conversion of I_2/I^- (2eZIBs) with a potential of 1.28 V vs. Zn^{2+}/Zn, offering an energy density of 290 Wh $kg_{I_2}^{-1}$, which is comparable to that of V_2O_5 cathodes (around 300 Wh kg^{-1}) but still lower than that of one-electron MnO_2 cathodes (around 420 Wh kg^{-1}).[17–19] Fortunately, high-valence I^+ can be activated, and it is reversible between I_2 and I^+ in aqueous electrolyte. When coupled with the I_2/I^- conversion, a doubled capacity of 422 mAh g^{-1} can be achieved in iodine electrodes based on

a four-electron conversion involving $I^+/I_2/I^-$ redox couples (4eZIBs), offering an impressive energy density up to 630 Wh $kg_{I_2}^{-1}$, which surpasses that of most prevailing cathodes for AZBs (Fig. 1b). While the electro-oxidation of iodine leads to the thermodynamically favorable generation of I^+ interhalogens in the presence of nucleophilic species such as halides or cyanide,[20] their stability is significantly compromised by hydrolysis. This occurs due to nucleophilic attack by hydroxyl groups, which degrades the reversibility of the 4e $I^+/I_2/I^-$ redox reactions in aqueous electrolytes.[21,22] Simultaneously, the sustained operation of Zn anodes in aqueous electrolytes is impeded by hydrogen evolution, interfacial corrosion, and dendrite growth, which progressively deplete the electrolyte over extended cycling.[23–26] These detrimental mechanisms synergistically diminish the coulombic efficiency (CE), induce voltage hysteresis, and degrade the long-term cycling stability of ZIBs. Prior research has predominantly focused on optimizing the reversibility of the Zn anode through various approaches and enhancing the two-electron I_2/I^- redox efficiency in ZIBs, yielding notable advancements.[27,28] However, research on high-valent iodine transformations currently remains at a nascent stage, and the understanding of the working mechanism and strategies for enhancing reversibility in $I^+/I_2/I^-$ conversion is still incomplete.

This perspective aims to highlight the significant potential of 4eZIBs with $I^+/I_2/I^-$ conversion for large-scale energy storage devices compared with traditional 2eZIBs with I_2/I^- conversion. It provides a concise introduction to the reaction mechanisms of the I_2/I^- and I^+/I_2 redox couples in aqueous electrolyte, followed by a comprehensive review of the activation and stabilization mechanisms of I^+ species. Finally, it discusses the remaining challenges and opportunities for practical high-energy aqueous 4eZIBs, alongside future development perspectives for this rapidly evolving field.
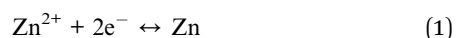
Chaofeng Zhang

Dr Chaofeng Zhang is currently a professor at the Institutes of Physical Science and Information Technology, Anhui University, Hefei, China. He received his BSc and MSc degrees from Lanzhou University and Fudan University, respectively. Then, he obtained his PhD degree in 2013 from the University of Wollongong, Australia. He completed a post-doctoral fellowship at the National Institute of Advanced Industrial Science and Tech-nology (AIST), Japan. His research focuses on electrochemistry for batteries, especially organic battery materials and electrolytes of aqueous zinc-ion batteries.

2. Fundamentals of the I_2/I^- and I^+/I_2 redox couples

Iodine cathodes are particularly promising in AZBs. The I_2 utilization rate and redox conversion efficiency play a crucial

role in the energy storage and release processes of ZIBs. The two-electron I_2/I^- transformation maintains high reversibility and fast kinetics, but suffers from intrinsic energy density constraints and polyiodide migration. In contrast, the four-electron $I^+/I_2/I^-$ process achieves a higher energy density, but it also presents more severe challenges. This section provides a concise introduction to the fundamental background of I_2 redox reactions, covering the mechanistic reactions of the I_2/I^- and I^+/I_2 redox couples, as well as the key challenges associated with these processes.

2.1 Typical I_2/I^- conversion

The earliest documented rechargeable zinc–iodine battery dates back to 1984.[29] In addition to employing a nylon-6-carbon cathode, a zinc plate anode, and a ZnI_2 electrolyte, a cation exchange membrane was utilized as a separator due to the high solubility of reaction intermediates (I_3^- or I_5^-) in aqueous solution. The specific electrochemical reactions can be described using the following equations:

Anode:

$$Zn^{2+} + 2e^- \leftrightarrow Zn \tag{1}$$

Cathode:

$$2I^- \leftrightarrow I_2 + 2e^- \tag{2}$$

or (after charging to some extent)

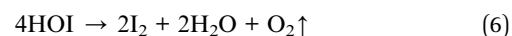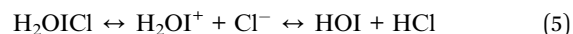$$I_3^- \leftrightarrow 3/2I_2 + e^- \tag{3}$$

The high solubility of polyiodides, particularly I_3^-, in aqueous electrolytes facilitates rapid reaction kinetics and outstanding rate performance, which is attributed to the liquid-phase reaction mechanism. However, the dissolution of I_3^- allows its migration across the separator to the anode compartment, where it undergoes spontaneous reduction with metallic Zn ($I_3^- + Zn \rightarrow Zn^{2+} + 3I^-$), resulting in irreversible energy loss—a phenomenon commonly referred to as the "shuttle effect" (Fig. 2a). Concurrently, the generated I^- ions, which remain highly mobile in aqueous solutions, can diffuse back to the cathode and participate in iodine oxidation. These continuous shuttling reactions significantly degrade battery reversibility, leading to diminished CE. Furthermore, the undesirable redox interactions between migrating polyiodides and Zn anodes induce severe Zn dissolution and surface passivation, leading to irreversible depletion of electroactive Zn and consequently compromising the cycle stability of 2eZIBs (Fig. 2b). Crucially, under Zn-limited conditions, this degradation process is exacerbated, presenting a critical bottleneck for the practical deployment of 2eZIBs. Moreover, the intrinsic side reactions of the Zn anode in aqueous electrolytes (including corrosion, hydrogen evolution, and byproduct formation), coupled with the persistent polyiodide shuttle effect continue to impose major constraints on the operational lifespan of ZIBs.[30–32]

To address these challenges, researchers have employed multiple strategies—including cathode host design,[15,33,34] electrolyte engineering,[35–38] electrode interface protection,[39,40] and separator modification[41,42]—yielding substantial advances. However, with the continuous development of aqueous-based batteries, the relatively low energy density provided by the two-electron-transfer I_2/I^- redox reaction diminishes the inherent advantages of iodine cathodes. Meanwhile, research focus has shifted toward activating the higher-valent iodine redox chemistry, aiming to exploit the multi-electron transfer capability of iodine and thereby significantly enhance the energy density of Zn–I_2 batteries.

2.2 High energy I^+/I_2 redox couple

Early studies conducted by Kolthoff and Jordan systematically studied the oxidation of iodide, indicating that under specified conditions iodide gives two anodic waves: the first corresponding to the formation of elementary iodine (I_2) and the second to unipositive iodine (I^+).[20] The presence of I^+ can be ascribed to the formation of charge-transfer complexes between electrophilic I^+ and nucleophilic species like halides, cyanide, and amines (Fig. 2c). When coupled with the Zn anode, the I^+/I_2 couple delivers a high discharge potential up to 1.8 V *vs.* $Zn^{2+}/$ Zn, highlighting its potential to deliver high energy density. Although the electro-oxidation of iodine leads to the thermodynamically favorable generation of I^+ interhalogens in the presence of nucleophilic species, their stability is significantly compromised by hydrolysis in aqueous media. For instance, ICl inevitably undergoes hydration by water, resulting in the formation of H_2OICl.[43] The lone-pair electrons of the oxygen atom in the water molecule readily donate electrons to form the hydrate complex. The hydration of H_2OICl can lead to deprotonation or disproportionation, resulting in the formation of HIO through the following reactions:

$$H_2OICl \leftrightarrow HOI + HCl \tag{4}$$

$$H_2OICl \leftrightarrow H_2OI^+ + Cl^- \leftrightarrow HOI + HCl \tag{5}$$

$$4HOI \rightarrow 2I_2 + 2H_2O + O_2\uparrow \tag{6}$$

This typically results in poor reversibility of iodine charge-transfer complexes in aqueous-based batteries.

Additionally, in contrast to the I_2/I^- conversion, the I^+/I_2 conversion critically relies on the formation of charge-transfer complexes between I^+ ions and nucleophilic species. The kinetically sluggish mass transport of these nucleophilic species within the electrode compromises the contribution of the I^+/I_2 redox reaction in practical battery systems, particularly under elevated active mass loading conditions (Fig. 2d). On the other hand, cross-parasitic reactions between the I_2/I^- and I^+/I_2 redox couples deteriorate battery performance. Specifically, incomplete polyiodide conversion during the I_2/I^- transformation neutralizes I^+ species generated from I^+/I_2 conversion, ultimately exacerbating the reversibility degradation of 4eZIBs.[44] Consequently, high-performance 4eZIBs must not only mitigate polyiodide shuttling, which is similar to that in
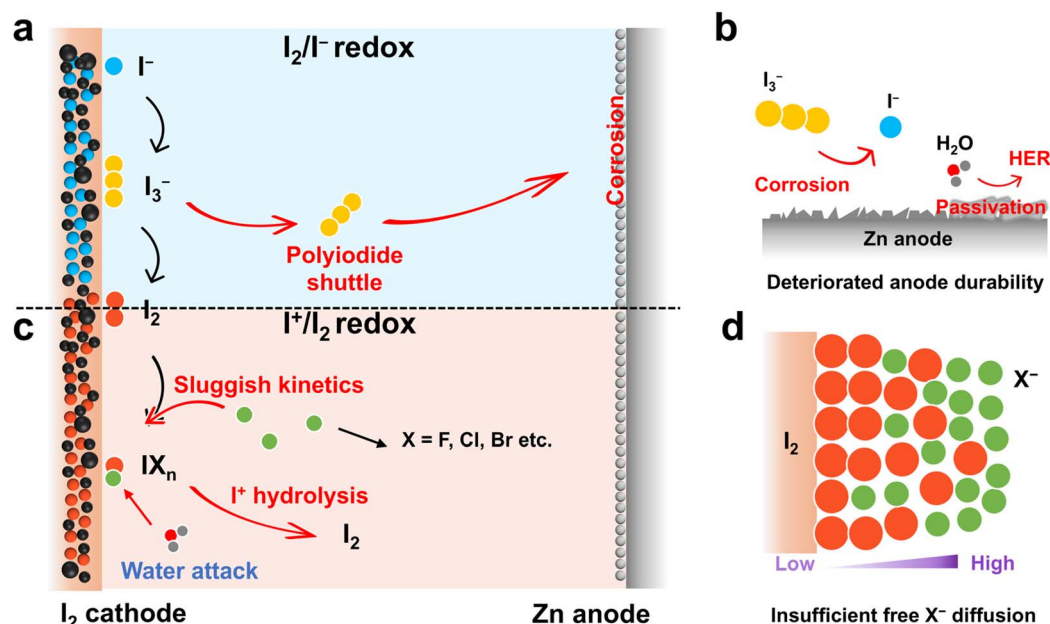
Fig. 2 Reaction mechanism and critical issues for (a and b) I_2/I^- conversion and (c and d) I^+/I_2 conversion in aqueous ZIBs.

2eZIBs, but also address the hydrolysis of I^+ species and the sluggish reaction kinetics among diverse iodine intermediates (Fig. 2).

3. Strategies for stabilizing the I^+ species for 4eZIBs

As delineated previously, zinc–iodine batteries leveraging four-electron $I^+/I_2/I^-$ redox chemistries confront more formidable challenges compared to their two-electron counterparts. Consequently, devising effective mitigation strategies entails compounded complexities. This section critically analyzes intervention strategies targeting cyclability limitations in 4eZIBs, encompassing electrolyte engineering, spatially confined catalysis, and coordination structure cathodes, providing guidance for designing high-performance 4eZIBs. Table 1 presents the key parameters and electrochemical performance of 4eZIBs optimized through different strategies, along with the performance benchmarks of 2eZIBs for comparative analysis.

3.1 Electrolyte engineering

Achieving four-electron transfer of iodine first requires the activation of monovalent I^+ species in aqueous electrolytes. As previously mentioned, this necessitates nucleophilic species in the electrolyte to form charge-transfer complexes with electrophilic I^+, thereby stabilizing the I^+/I_2 conversion process. Halide ions X^- (X = F, Br, and Cl), common nucleophiles, have been employed for the first time in Zn–I_2 batteries to stabilize I^+ species through the formation of interhalogen compounds (Fig. 3a).[45] The findings demonstrate that Cl^- exhibits superior efficacy compared to F^- in activating and stabilizing the I^+/I_2 redox reaction. Furthermore, introducing alkali metal chlorides

into the electrolyte significantly enhances the reaction reversibility and kinetics of the I^+/I_2 conversion. This performance enhancement is primarily attributable to two synergistic mechanisms: (1) the I^+/I_2 conversion involving nucleophilic halide ions follows a reaction mechanism analogous to that of dual-ion batteries, where the reaction equilibrium depends on halide ion concentration in the electrolyte. Specifically, elevated halide concentrations thermodynamically favor the conversion of I_2 to I^+. (2) The introduction of alkali metal cations further reduces the energy barrier for this conversion reaction, with K^+ demonstrating optimal catalytic efficacy.

However, I^+ species demonstrate pronounced hydrolysis propensity in aqueous electrolytes under high water activity conditions. This hydrolysis equilibrium of interhalogen compounds can be effectively suppressed in electrolyte systems featuring reduced water chemical potential, elevated halide (X^-) concentrations, and enhanced proton activity (Fig. 3b). For example, Liang *et al.* proposed a Cl^- based highly concentrated electrolyte consisting of $ZnCl_2$, LiCl, and acetonitrile (ACN) in a molarity ratio of 19 : 19 : 8 to improve the reversibility of $I^+/I_2/I^-$ conversions.[21] This concentrated electrolyte configuration delivered abundant mobile Cl^- that effectively catalyzed the iodide redox conversion, yielding a reversible capacity of 594 mAh g^{-1}.

Concomitantly, the solvent network population was substantially depleted within this electrolyte matrix, kinetically suppressing I^+ hydrolysis. Consequently, the resultant 4eZIBs exhibited exceptional long-term cyclability, sustaining 6000 cycles with negligible degradation at 2 A g^{-1}. However, significant challenges associated with highly concentrated electrolytes, including elevated viscosity that hinders ion transport and results in sluggish electrode kinetics, should be noted (Fig. 3c). While reducing the halogen content in the electrolyte can

Table 1 Summary of various Zn–I$_2$ battery systems and their performance

Cathode materials	Electrolyte	Loading (mg cm^{-2})	Capacity (mAh g^{-1})	Performance	Energy (Wh kg^{-1})	Ref.
Traditional 2e$^-$ conversion						
I$_2$@Nb$_2$CT$_x$	1 M ZnSO$_4$	—	205$_{I_2}$	80% (23 000 cycles)	259.3$_{I_2}$	34
I$_2$@AC	AMPS hydrogel	1.4	209$_{I_2}$	100% (14 000 cycles)	250.8$_{I_2}$	36
Energy dense 4e$^-$ conversion						
Ti$_3$C$_2$I$_2$	2 M ZnCl$_2$ 1 M KCl	1.0–1.5	207$_{Ti_3C_2I_2}$	80% (2800 cycles)	280$_{Ti_3C_2I_2}$ 467$_{I_2}$	45
I$_2$/PAC	19 M ZnCl$_2$ 19 M LiCl 8 M ACN	4.0–5.0	594$_{I_2}$	82% (6000 cycles)	750$_{I_2}$	21
I$_2$@AC	1.17 M ZnSO$_4$ 0.78 M ChCl 3 M Gly	1.0	572$_{I_2}$	76% (15 000 cycles)	770$_{I_2}$	46
I$_2$/Fe$_{SA}$–NC	19 M ZnCl$_2$ 19 M LiCl 8 M ACN	10.0	513.2$_{I_2}$	80% (10 000 cycles)	653.8$_{I_2}$	50
Ni–Fe–I LDH	1 M ZnSO$_4$ 0.2 M ZnBr$_2$	—	350$_{I_2}$	94.6% (10 000 cycles)	—	53
CuPc@CNT–ZnI$_2$	3 M ZnSO$_4$	3.0	229$_{ZnI_2}$	64.8% (1000 cycles)	233.8$_{ZnI_2}$	51
Hexy$_4$NICl$_2$	3 M ZnSO$_4$ 1 M ZnCl$_2$	2.0	445$_{I_2}$	75% (1200 cycles)	—	56
ODASnI$_4$	2 M ZnSO$_4$ 0.5 M LiCl	1.0–1.1	421$_{I_2}$	60% (500 cycles)	215$_{ODASnI_4}$	57
(BAD)BiI$_4$	2 M ZnSO$_4$ 2 M LiCl	0.9–1.2	434$_{I_2}$ 263$_{(BAD)BiI_4}$	78% (10 000 cycles)	210$_{(BAD)BiI_4}$	40

alleviate the aforementioned issues, the HER/OER caused by high water activity gradually becomes more prominent. Consequently, reconstructing the hydrogen-bonding network of water in low-halogen-concentration electrolytes is necessary to suppress its reactivity. Recently, Guo *et al.* developed a low-halogen-concentration eutectic electrolyte—comprising cost-
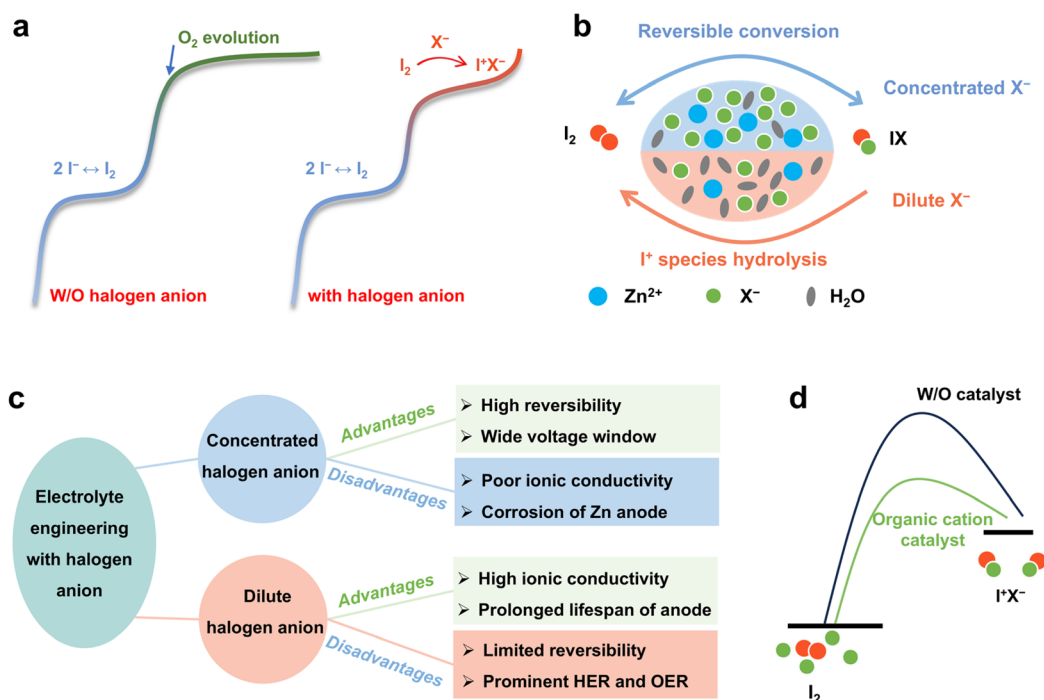

Fig. 3 Activating and stabilizing I$^+$ in halogen-based electrolytes. (a) Illustration of the I$_2$ conversion with/without the assistance of halogen anions. (b) The influence of halogen concentration on the reaction of the I$^+$/I$_2$ couple. (c) Advantages and disadvantages of electrolyte with concentrated or dilute halogen anions respectively. (d) Schematic diagram of the energy barrier for I$^+$/I$_2$ conversion with an organic cation catalyst.

effective $ZnSO_4$, choline chloride (ChCl), and glycerol (Gly)—significantly enhancing the kinetics of $I^+/I_2/I^-$ conversions.[46] Specifically, iodophilic Ch^+ exhibit synergistic interactions with glycerol, substantially stabilizing I^+ intermediates while accelerating iodine redox kinetics (Fig. 3d). Moreover, eutectic component–water coordination perturbs the organization of free-water H-bonds, enhancing electrolyte cryogenic resilience. Consequently, 4eZIBs incorporating this optimized hydrated eutectic electrolyte manifest exceptional cycling stability (<0.0016% capacity decay/cycle over 15 000 cycles) and maintain operational functionality across an extended thermal range (−25 to 40 °C). It is noteworthy that some electrophilic reagents, including nicotinamide,[47] urea,[48] and analogous structural motifs, can also stabilize the I^+/I_2 redox couple *via* coordination stabilization effects.

Beyond conventional liquid electrolytes, hydrogel electrolytes with programmable molecular architectures and precise moisture-regulating capabilities play pivotal roles in advancing Zn–I_2 batteries. Zhang *et al.* engineered a polycationic hydrogel electrolyte, bacterial cellulose/p(AM-*co*-VBIMBr) (denoted as BAVBr), that facilitates and stabilizes high-valent I^+/I_2 redox conversion through tailored coordination environments.[49] The Br species in BAVBr hydrogel activates the high voltage I^+/I_2 redox reaction by forming negative charged interhalogens (IBr_2^- and IBr_3^-), and then these species are stabilized by the positively charged $-NR_3^+$ units in BAVBr through strong electrostatic interactions. Benefiting from this intelligent molecular engineering paradigm, full cells assembled with the BAVBr hydrogel electrolyte demonstrate ultralong cyclability at a low concentration of halide (1 M Br^-), sustaining over 14 000 cycles at 3 A g^{-1} with minimal capacity decay.

3.2 Spatially confined catalysis

In addition to the polyiodide shuttle challenge inherent in their reaction processes in 2eZIBs, the pronounced hydrolysis tendency of I^+ ions and the sluggish kinetics of interhalogen compound conversion remain critical issues in 4eZIBs. Conventional carbon materials, leveraging their high electrical conductivity and porous architecture, have successfully served as effective hosts for iodine cathodes while spatially confining the polyiodide shuttle. However, such simplistic physical

confinement fails to adequately suppress the hydrolysis of I^+ ions. In contrast, metal-based coordination frameworks afford strengthened electrostatic binding with I^+ species, thereby serving as an imperative mechanism for improved reversibility in the conversion reaction. Moreover, these metal active sites often exhibit catalytic activity toward the iodine conversion reaction. Coupled with the porous carbon substrate, this synergy significantly enhances the reaction kinetics of $I^+/I_2/I^-$ conversion. Currently, various porous carbon-supported metal-based catalysts, including single-atom catalysts,[50] metal-phthalocyanine compounds,[51] Co_9S_8@nitrogen-doped-carbon,[52] and Ni–Fe LDH[53] have been developed, yielding marked improvements in battery performance (Fig. 4a). Illustrative of this approach, Liang *et al.* reported an Fe single-atom catalyst featuring dense $Fe-N_4$ coordination sites for 4eZIBs.[50] Their analysis revealed that p–p orbital coupling between iron centers and iodine species enhances I^+ adsorption affinity, thereby suppressing hydrolytic decomposition through elevated energy barriers for proton dissociation from the $ICl·H_2O$ intermediate. Concomitantly, d–p orbital hybridization promotes inter-iodide electron transfer kinetics, accelerating redox conversions. Consequently, such catalysts enable 4eZIBs exhibiting near-unity coulombic efficiencies (>99%) at practical areal capacities exceeding 3 mAh cm^{-2}, alongside exceptional cycling stability (>10 000 cycles at 2 A g^{-1}). Notably, I_3^- shuttle effects during I_2/I^- reactions trigger comproportionation with I^+ species, accelerating cell degradation. Hence, strategic catalyst design must prioritize dual objectives: facilitating I_2/I^- kinetics to mitigate I_3^- formation and stabilizing I^+ intermediates to enhance I^+/I_2 reversibility.

Layered Double Hydroxides (LDH) facilitate rapid electron transport through their distinctive layered architecture, rendering them well-established materials for diverse applications in electrocatalysis and electrochemical electrodes. As an example, Ni–Fe–I LDH electrode has been synthesized and used as the host for $I^+/I_2/I^-$ redox reactions.[53] The large and stable interlayer distance of Ni–Fe LDH enables the redox reactions of $I^+/I_2/I^-$ to occur within the interlayer, which effectively inhibits the shuttling of iodide species. Very recently, Lu *et al.* engineered a copper phthalocyanine/graphene heterostructure (CuPc@rGO) for iodine confinement, substantially stabilizing
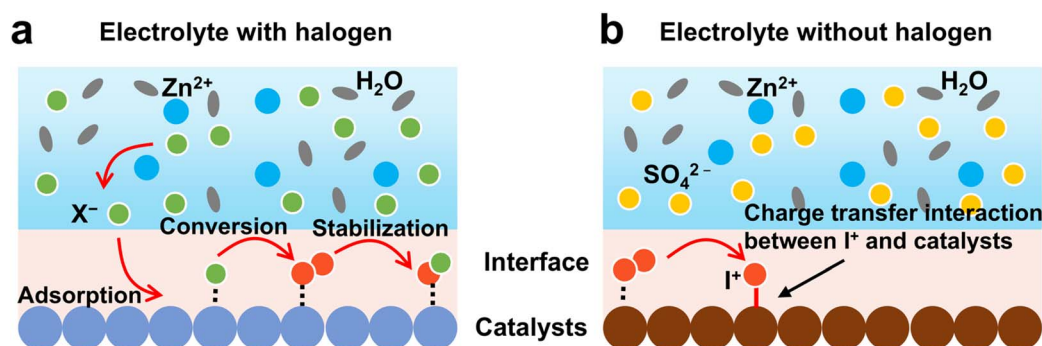

Fig. 4 Stabilizing I^+ through catalysts. (a) Catalytic effect of I^+/I_2 conversion in halogen-based electrolytes. (b) Activating and stabilizing I^+ in halogen free electrolytes.

the multi-step $I^+/I_2/I^-$ redox pathway in aqueous halide-free $ZnSO_4$ electrolytes.[51] The study demonstrated that the stabilization of I^+ cations arises from charge-transfer-mediated interactions with CuPc within the confinement matrix (Fig. 4b). Crucially, π-conjugation-induced electron delocalization from CuPc to the carbon framework in heterostructured hosts synergistically amplifies this stabilization mechanism, thereby enabling highly reversible $I^+/I_2/I^-$ redox cycling in Zn–I_2 batteries. This study introduces a novel approach for achieving high-voltage iodine redox chemistry in aqueous electrolytes without halide ions. However, the efficacy of this strategy, which relies on charge interactions between the catalyst and I^+ to activate I^+, remains to be validated under conditions of high electrode loading or when the iodine mass fraction exceeds that of the catalyst.

3.3 Coordination structure cathodes

Previous studies have documented the capability of quaternary ammonium cations (Q^+) to engage in complex formation with polyhalide species such as I_3^- and Br_3^-.[54,55] This complexation mechanism has been experimentally corroborated in halogen-based battery systems utilizing I_2/I^- and Br_2/Br^- redox electrochemistry. In 4eZIBs, typically in X^--rich environments, I^+ species can form IX_2^- anions (e.g. IBr_2^- or ICl_2^-). Therefore, the formation of complexes between anionic IX_2^- species and quaternary ammonium cations represents a viable strategy for stabilizing I^+ ions. Liang et al. investigated the complexation of ICl_2^- by quaternary ammonium cations with varying alkyl chain lengths, and studied the electrochemical performance of Q–ICl_2 complexes as cathodes for 4eZIBs (Fig. 5a).[56] The results revealed enhanced Q–ICl_2 binding energies and improved aqueous

stability of the resultant complexes with increasing chain length. This phenomenon is attributable to the similarity–intermiscibility principle, wherein extended alkyl chains progressively enhance the lipophilic and hydrophobic character of Q–ICl_2 complexes. This approach mitigated the hydrolysis/dissolution of the I^+ species, leading to superior rate capability and an extended lifespan of 4eZIBs within a dilute aqueous electrolyte. Despite the exceptional efficacy of elongated spacer cations in stabilizing I^+ species, their pronounced mass fraction detrimentally compromises the cathodic energy density. Further optimization of the ammonium salts with asymmetric structures or smaller molecular weights is necessary.

Metal-halide perovskites adopting the ABX_3 architecture ($A = Cs^+$, $CH_3NH_3^+$, $HC(NH_2)_2^+$; $B = Pb^{2+}$, Sn^{2+}; $X = I^-$, Br^-, Cl^-) represent viable alternatives for conversion-type iodide cathodes due to their suitable ionic bonding strength for halogen anions at X-sites (Fig. 5b). The implementation of diammonium cations at A-sites in low-dimensional derivatives confers enhanced moisture stability, advancing these materials toward practical deployment. In such systems, diammonium spacers generate a confinement effect that immobilizes active species and mitigates the shuttling of intermediate anions through positive charged functional groups. Leveraging these advantages, select perovskite-structured iodide cathodes, exemplified by $ODASnI_4$ (ref. 57) and (BAD)BiI_4,[40] demonstrate amplified electrochemical performance in zinc–iodine batteries with $I^+/I_2/I^-$ conversion. While the strategy of chemically binding halogen intermediates effectively suppresses their hydrolysis, this solid–solid phase transformation reaction compromises the inherent kinetic advantages of the system. Furthermore, the formation of complexes or the presence of substantial non-active species (such as organic cations or metal components) in the perovskite structure leads to
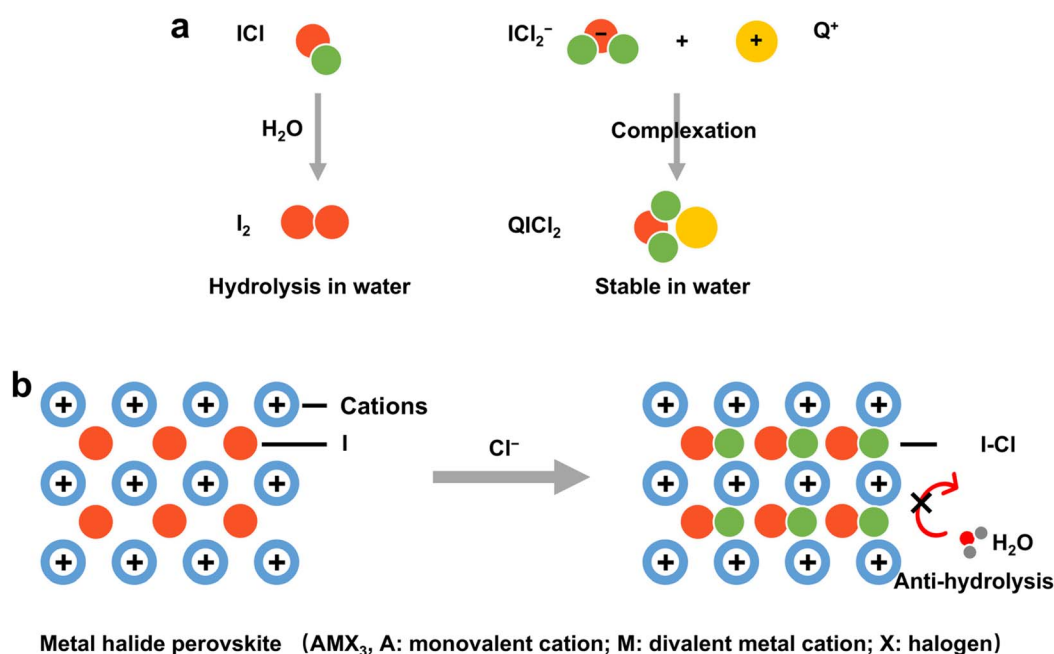

Fig. 5 Confine iodine through coordination chemistry. (a) Schematic diagram of the complexation of quaternary ammonium salts (Q^+) with ICl_2^- in aqueous media. (b) Schematic illustration of iodine oxidation at perovskite type electrodes.
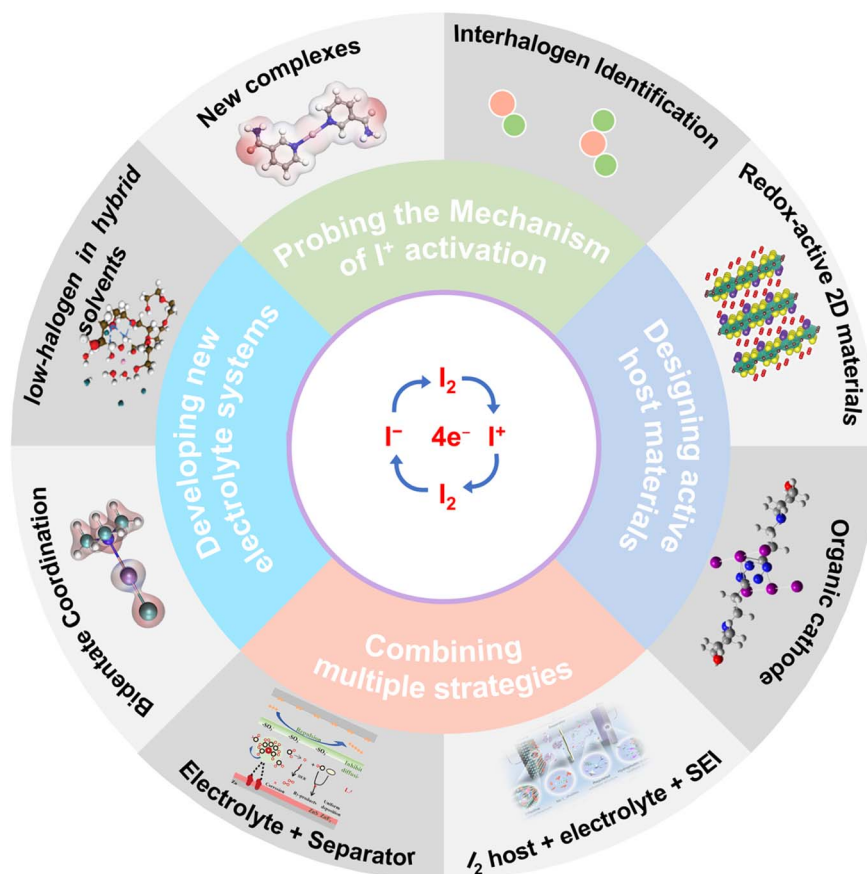
Fig. 6 Feasible strategies to enhance the reversibility of $I^+/I_2/I^-$ in 4eZIBs.

a reduction in electrode energy density. Therefore, the pursuit of enhanced cathodic energy density necessitates increasing the iodine mass fraction in iodide-rich complex cathodes.

4. Conclusion and outlook

In contrast to the traditional two-electron conversion Zn–I_2 battery, the 4eZIBs with four-electron transfer of the $I^+/I_2/I^-$ redox couple deliver a duplicate theoretical capacity of 422 mAh g^{-1}, offering substantial potential for improved energy density. However, they are hampered by the poor redox reversibility of I^+/I_2 conversion process caused by the shuttle effect of iodide intermediates and the strong hydrolysis tendency of I^+ species in aqueous electrolytes. In addition to providing a fundamental understanding of the I_2/I^- and I^+/I_2 conversions, we present a comprehensive overview of the recently strategies focused on improving the battery performance of 4eZIBs. Rather than providing a conclusive set of studied, this perspective advocates that the field continue to examine research on how to enhance the reversibility of the I^+/I_2 redox couple, and proposes some specific feasible strategies (Fig. 6).

4.1 Probe the conversion mechanism of I^+/I_2 in greater depth

Among the studied chelating agents capable of realizing the reversible I^+/I_2 redox reaction *via* I^+ chelation, halogen-based chelators currently appear to represent the most straightforward and controllable strategy. However, their development remains at an early exploratory stage, and the underlying reaction mechanisms have yet to be clearly elucidated. Firstly, in bromide-containing electrolytes, it remains unclear whether molecular iodine (I_2) generated during charging forms an I_2Br^- complex with bromide before further oxidation to IBr_2^-; and in chloride-containing electrolytes, whether the species chelated with I^+ is ICl or ICl_2^-. Elucidating the precise chelation form of I^+ is pivotal for developing enhanced strategies to promote the reversibility of the I^+/I_2 redox reaction. For example, I_2Br^- or ICl_2^- anion intermediates can be coordinated with functional cations to inhibit their hydrolysis. Secondly, elucidating the reaction pathways and intermediate species is crucial for guiding the design of iodine host materials to enhance the kinetics of the I^+/I_2 redox conversion. Furthermore, it is essential to determine whether specific stoichiometric ratios exist between halogen chelators and iodine active species. For instance, what is the minimum required concentration of halogen in the electrolyte to achieve reversible I^+/I_2 conversion in a cathode with a specific iodine loading? This understanding is paramount for developing zinc–iodine batteries with high areal capacity and represents an indispensable prerequisite for their successful industrial implementation. Finally, whether nucleophiles more effective than halogens exist that can yield more stable charge-transfer complexes with I^+ also merits

further rigorous investigation. Addressing this question is crucial for advancing alternative strategies to enhance the reversibility of the I^+/I_2 redox couple.

4.2 Design cathode host matrices with electrochemical activity

The inherently low electrical conductivity of iodine and the formation of soluble intermediates during redox reactions necessitate the development of efficient host architectures. While porous carbon materials and layered 2D materials represent conventional iodine hosts, these electrochemically inert constituents typically constitute substantial weight fractions (>40%) in cathodes, severely compromising the high specific energy advantages otherwise achievable through multi-electron iodine redox chemistry. Huang *et al.* presented a layered MBene with ordered metal vacancies and –Br terminal groups to host I_2, denoted as MBene–Br.[58] This cathode without I_2 hosting delivered a high discharge capacity of 143.8 mAh g^{-1} based on the mass of MBene–Br, benefiting from the introduction of the Br^0/Br^- redox reaction from the –Br terminations, outperforming the MBenes with typical pseudocapacitive behavior. Finally, a high capacity of 405 mAh g^{-1} was achieved when coupled with I_2/I^- conversion, offering a recorded specific energy of 485.8 Wh kg^{-1} (based on the mass of I_2@MBene–Br). Combining the iodine redox chemistry with an organic cathode based on the Zn^{2+}/H^+ co-intercalation mechanism is another optional strategy to improve the energy density of the whole cathode. For example, Shu *et al.* developed a diquinoxalino[2,3-*a*:2′,3′-*c*]phenazine (HATN)@CMK-3 composite as the cathode and 0.5 M $Zn(OTf)_2$ + 50 mM ZnI_2 hybrid solution as the electrolyte for an aqueous zinc battery.[59] The HATN@CMK-3 with C=N groups not only stores Zn^{2+} and H^+ ions at low potential but also acts as a substrate to promote the conversion reaction of I_2/I^- at high potential. Additionally, the N-functional groups in HATN show strong interaction with I_3^- intermediates due to Lewis base interactions, thus greatly limiting the shuttle of I_3^-.

The aforementioned iodine host materials merely function by coupling active electrodes with the I_2/I^- redox pair, while their potential inhibitory effects on I^+ hydrolysis remain unexplored. Nevertheless, this paradigm shift provides an insightful foundation for harnessing four-electron $I^+/I_2/I^-$ redox chemistry.

4.3 Develop new electrolyte systems

Functioning as the conductive medium for charge carriers, the electrolyte not only establishes the essential bridge for ion transport between the cathode and anode, but also exerts a critical influence on the interfacial electrochemical behavior at the electrode surfaces. This consequently impacts both the energy storage performance and safety profile of the battery. Compared to strategies focusing solely on zinc anode interface protection or cathode host design, electrolyte-based approaches offer relative simplicity and the capacity to simultaneously address both electrodes. Furthermore, considering the operational demands of energy storage devices under practical conditions, such as extreme environments involving elevated or sub-ambient

temperatures, electrolyte optimization becomes imperative. This necessity arises from the pronounced temperature susceptibility inherent in traditional aqueous electrolytes.

Within the previously reviewed strategies utilizing electrolytes to activate and stabilize the I^+/I_2 conversion, the potential of 4eZIBs is constrained by the limitations of high-concentration and eutectic electrolytes, namely their lower ionic conductivity and cost-effectiveness concerns. Although gel electrolytes demonstrate improved performance in multi-electron Zn–I_2 batteries, their application scope is predominantly oriented towards flexible devices, offering less advantage for large-scale energy storage. In contrast, low-concentration halogen electrolytes matched with electrolyte additives, which are capable of coordinating or complexing with I^+ ions, appear to be a more promising strategy to effectively inhibit the hydrolysis of I^+ ions.[60,61] Additionally, this strategy maintains the high ionic conductivity advantage of aqueous electrolytes, while simultaneously providing greater versatility in electrolyte formulation design. It should be noted that when designing such electrolytes, the electrochemical behavior of the electrolytes at high or low temperatures cannot be ignored. A viable strategy entails introducing organic co-solvents into the electrolyte, thereby simultaneously enhancing its temperature tolerance while suppressing side reactions triggered by active water.

4.4 The synergy of multiple strategies

For 4eZIBs, the challenges extend beyond the iodine cathode-related shuttle effect and I^+ ion hydrolysis to include non-negligible adverse reactions at the Zn anode. While single-strategy approaches often struggle to concurrently address all issues in Zn–I_2 systems, the implementation of synergistic multi-strategy methodologies tailored to specific problems represents a highly viable approach. Previous research has demonstrated the application of this collaborative strategy to enhance the reversibility of the I_2/I^- conversion reaction, yielding remarkably promising outcomes. For instance, Zhang *et al.* illustrated the synergistic effect between an electrolyte additive and a separator on stabilizing the interface in Zn–I_2 batteries.[28] Presented as a notable case study, the researchers employed an efficient and cost-effective additive, sodium lignosulfonate (LAS), in conjunction with a flexible sulfonated poly(ether sulfone) membrane. This combination facilitated the formation of a stable solid electrolyte interphase (SEI) on the zinc anode and mitigated the polyiodide shuttling effect through electrostatic repulsion exerted by the $R–SO_3^-$ groups anchored on the separator membrane. Recently, Lin *et al.* proposed a tripartite synergistic optimization strategy involving an MXene cathode host, an *n*-butanol electrolyte additive, and *in situ* solid electrolyte interphase protection.[62] These studies offer a promising strategy for the subsequent research to comprehensively improve battery performance.

Author contributions

R. W., Q. M., and P. X. provided support for format analysis. Y. L., L. Z. and C. Z. acquired funding. C. Z. reviewed and refined the manuscript.

Conflicts of interest

There are no conflicts to declare.

Data availability

No primary research results, software or code have been included and no new data were generated or analysed as part of this review.

Acknowledgements

Notes and references

1 S. Chu and A. Majumdar, *Nature*, 2012, **488**, 294.

2 B. Dunn, H. Kamath and J.-M. Tarascon, *Science*, 2011, **334**, 928.

3 L. Zhang, R. Wang, Z. Liu, J. Wan, S. Zhang, S. Wang, K. Hua, X. Liu, X. Zhou, X. Luo, X. Zhang, M. Cao, H. Kang, C. Zhang and Z. Guo, *Adv. Mater.*, 2023, **35**, e2210082.

4 J. B. Goodenough and Y. Kim, *Chem. Mater.*, 2010, **22**, 587.

5 Y. Liu, M. Lei, C. Lai, J. Meng, X. Wu, Y. Yu, Y. Zhang and C. Li, *Mater. Today*, 2022, **61**, 65.

6 J. F. Parker, C. N. Chervin, I. R. Pala, M. Machler, M. F. Burz, J. W. Long and D. R. Rolison, *Science*, 2017, **356**, 415.

7 J. Wan, R. Wang, Z. Liu, L. Zhang, F. Liang, T. Zhou, S. Zhang, L. Zhang, Q. Lu, C. Zhang and Z. Guo, *ACS Nano*, 2023, **17**, 1610.

8 H. Li, M. Cao, Z. Fu, Q. Ma, L. Zhang, R. Wang, F. Liang, T. Zhou and C. Zhang, *Chem. Sci.*, 2024, **15**, 4341.

9 H. Li, M. Cao, R. Wang, P. Xiong, Y. Liu, L. Zhang, L. Zhang, L. Zhang, D. Chao and C. Zhang, *Angew. Chem., Int. Ed.*, 2025, **64**, e202508057.

10 H. Pan, B. Li, D. Mei, Z. Nie, Y. Shao, G. Li, X. S. Li, K. S. Han, K. T. Mueller, V. Sprenkle and J. Liu, *ACS Energy Lett.*, 2017, **2**, 2674.

11 L. Hu, C. Dai, Y. Zhu, X. Hou, Z. Liu, X. Geng, H. Wang, J. Chen, N. Sun, Q. Rong, Y. Zhu, X. He and Y. Lin, *Energy Environ. Sci.*, 2024, **17**, 5552.

12 P. Li, S. Yang, J. Zhu, S. Wang, Y. Hou, H. Cui, Z. Chen, R. Zhang, Z. Wu, Y. Wang, Z. Wei, X. Liu, S. Zhang, X. Li and C. Zhi, *Matter*, 2024, **7**, 1867.

13 K. Hua, Q. Ma, Y. Liu, P. Xiong, R. Wang, L. Yuan, J. Hao, L. Zhang and C. Zhang, *ACS Nano*, 2025, **19**, 14249.

14 W. Wang, S. Zhang, L. Zhang, R. Wang, Q. Ma, H. Li, J. Hao, T. Zhou, J. Mao and C. Zhang, *Adv. Mater.*, 2024, **36**, 2400642.

15 S. J. Zhang, J. Hao, H. Li, P. F. Zhang, Z. W. Yin, Y. Y. Li, B. Zhang, Z. Lin and S. Z. Qiao, *Adv. Mater.*, 2022, **34**, e2201716.

16 C. Bai, F. Cai, L. Wang, S. Guo, X. Liu and Z. Yuan, *Nano Res.*, 2018, **11**, 3548.

17 H. Pan, Y. Shao, P. Yan, Y. Cheng, K. S. Han, Z. Nie, C. Wang, J. Yang, X. Li, P. Bhattacharya, K. T. Mueller and J. Liu, *Nat. Energy*, 2016, **1**, 16039.

18 Y. Yang, Y. Tang, G. Fang, L. Shan, J. Guo, W. Zhang, C. Wang, L. Wang, J. Zhou and S. Liang, *Energy Environ. Sci.*, 2018, **11**, 3157.

19 Y. Zeng, J. Xu, Y. Wang, S. Li, D. Luan and X. W. Lou, *Angew. Chem., Int. Ed.*, 2022, **61**, e202212031.

20 I. M. Kolthoff and J. Jordan, *J. Am. Chem. Soc.*, 1953, **75**, 1571.

21 Y. Zou, T. Liu, Q. Du, Y. Li, H. Yi, X. Zhou, Z. Li, L. Gao, L. Zhang and X. Liang, *Nat. Commun.*, 2021, **12**, 170.

22 W. Zong, J. Li, C. Zhang, Y. Dai, Y. Ouyang, L. Zhang, J. Li, W. Zhang, R. Chen, H. Dong, X. Gao, J. Zhu, I. P. Parkin, P. R. Shearing, F. Lai, K. Amine, T. Liu and G. He, *J. Am. Chem. Soc.*, 2024, **146**, 21377.

23 J. Wan, R. Wang, Z. Liu, S. Zhang, J. Hao, J. Mao, H. Li, D. Chao, L. Zhang and C. Zhang, *Adv. Mater.*, 2024, **36**, e2310623.

24 R. Wang, Q. Ma, L. Zhang, Z. Liu, J. Wan, J. Mao, H. Li, S. Zhang, J. Hao, L. Zhang and C. Zhang, *Adv. Energy Mater.*, 2023, **13**, 2302543.

25 L. Yuan, J. Hao, B. Johannessen, C. Ye, F. Yang, C. Wu, S.-X. Dou, H.-K. Liu and S.-Z. Qiao, *eScience*, 2023, **3**, 100096.

26 R. Wang, S. Xin, D. Chao, Z. Liu, J. Wan, P. Xiong, Q. Luo, K. Hua, J. Hao and C. Zhang, *Adv. Funct. Mater.*, 2022, **32**, 2207751.

27 W. Zhang, Y. Liu, X. Luo, R. Wang, K. Zhou, L. Yuan, F. Li, H. Li, L. Zhang and C. Zhang, *Adv. Funct. Mater.*, 2025, **35**, e12633.

28 R. Wang, Y. Liu, Q. Luo, P. Xiong, X. Xie, K. Zhou, W. Zhang, L. Zhang, H. J. Fan and C. Zhang, *Adv. Mater.*, 2025, **37**, 2419502.

29 T. Yamamoto, M. Hishinuma and A. Yamamoto, *Inorg. Chim. Acta*, 1984, **86**, L47.

30 Z. Liu, R. Wang, Y. Gao, S. Zhang, J. Wan, J. Mao, L. Zhang, H. Li, J. Hao, G. Li, L. Zhang and C. Zhang, *Adv. Funct. Mater.*, 2023, **33**, 2308463.

31 M. Zhang, H. Wei, Y. Zhou, W. Wen, L. Zhang and X.-Y. Yu, *Chem. Sci.*, 2024, **15**, 18187.

32 L. Zhang, J. Xiao, X. Xiao, W. Xin, Y. Geng, Z. Yan and Z. Zhu, *eScience*, 2023, **4**, 100205.

33 F. Yang, J. Long, J. A. Yuwono, H. Fei, Y. Fan, P. Li, J. Zou, J. Hao, S. Liu, G. Liang, Y. Lyu, X. Zheng, S. Zhao, K. Davey and Z. Guo, *Energy Environ. Sci.*, 2023, **16**, 4630.

34 X. Li, N. Li, Z. Huang, Z. Chen, G. Liang, Q. Yang, M. Li, Y. Zhao, L. Ma, B. Dong, Q. Huang, J. Fan and C. Zhi, *Adv. Mater.*, 2021, **33**, e2006897.

35 R. Wang, Z. Liu, J. Wan, X. Zhang, D. Xu, W. Pan, L. Zhang, H. Li, C. Zhang and Q. Zhang, *Adv. Energy Mater.*, 2024, **14**, 2402900.

36 Y. Liu, F. Li, J. Hao, H. Li, S. Zhang, J. Mao, T. Zhou, R. Wang, L. Zhang and C. Zhang, *Adv. Funct. Mater.*, 2024, **34**, 2400517.

37 C.-C. Kao, J. Liu, C. Ye, S.-J. Zhang, J. Hao and S.-Z. Qiao, *J. Mater. Chem. A*, 2023, **11**, 23881.

38 C. Dong, H. Ji, T. Yang, H. Wu, C. Liu, X. Xie, O. Sheng, D. Yang, T. Shen, Z. Sun, J. Zhang, R. Zheng, C. Zhang and X. Zhang, *Adv. Funct. Mater.*, 2025, **35**, e13529.

39 Z. Hu, X. Wang, W. Du, Z. Zhang, Y. Tang, M. Ye, Y. Zhang, X. Liu, Z. Wen and C. C. Li, *ACS Nano*, 2023, **17**, 23207.

40 J. Gong, H. Zhang, X. Liang, P. Li, Y. Liu, X. Li, C. Zhi, Z. Zhu, X. C. Zeng, N. Li and J. Xu, *Adv. Funct. Mater.*, 2024, **34**, 2411137.

41 Z. Li, X. Wu, X. Yu, S. Zhou, Y. Qiao, H. Zhou and S. G. Sun, *Nano Lett.*, 2022, **22**, 2538.

42 Y. Kang, G. Chen, H. Hua, M. Zhang, J. Yang, P. Lin, H. Yang, Z. Lv, Q. Wu, J. Zhao and Y. Yang, *Angew. Chem., Int. Ed.*, 2023, **62**, e202300418.

43 F. A. Philbrick, *J. Am. Chem. Soc.*, 1934, **56**, 1257.

44 C. L. Bentley, A. M. Bond, A. F. Hollenkamp, P. J. Mahon and J. Zhang, *Anal. Chem.*, 2016, **88**, 1915.

45 X. Li, M. Li, Z. Huang, G. Liang, Z. Chen, Q. Yang, Q. Huang and C. Zhi, *Energy Environ. Sci.*, 2021, **14**, 407.

46 L. Liu, L. Zhang, Y. Liu, S. Zhang, R. Wang, F. Li, H. Li, J. Hao, C. Zhang and Z. Guo, *Adv. Energy Mater.*, 2025, **15**, 2501460.

47 W. Li, H. Xu, H. Zhang, F. Wei, T. Zhang, Y. Wu, L. Huang, J. Fu, C. Jing, J. Cheng and S. Liu, *Energy Environ. Sci.*, 2023, **16**, 4502.

48 C. Li, H. Li, X. Ren, L. Hu, J. Deng, J. Mo, X. Sun, G. Chen and X. Yu, *ACS Nano*, 2025, **19**, 2633.

49 Y. Liu, L. Zhang, L. Liu, Q. Ma, R. Wang, P. Xiong, H. Li, S. Zhang, J. Hao and C. Zhang, *Adv. Mater.*, 2025, **37**, 2415979.

50 T. Liu, C. Lei, H. Wang, C. Xu, W. Ma, X. He and X. Liang, *Sci. Bull.*, 2024, **69**, 1674.

51 J. Kang, C. Wang, Z. Liu, L. Wang, Y. Meng, Z. Zhai, J. Zhang and H. Lu, *Energy Storage Mater.*, 2024, **68**, 103367.

52 T. Hu, Y. Zhao, Y. Yang, H. Lv, R. Zhong, F. Ding, F. Mo, H. Hu, C. Zhi and G. Liang, *Adv. Mater.*, 2024, **36**, e2312246.

53 C. Wang, X. Ji, J. Liang, S. Zhao, X. Zhang, G. Qu, W. Shao, C. Li, G. Zhao, X. Xu and H. Li, *Angew. Chem., Int. Ed.*, 2024, **63**, e202403187.

54 L. Gao, Z. Li, Y. Zou, S. Yin, P. Peng, Y. Shao and X. Liang, *iScience*, 2020, **23**, 101348.

55 X. Liao, Z. Zhu, Y. Liao, K. Fu, Y. Duan, L. Lv, L. Wu, W. Wang, X. He, K. Yang, P. Tian, W. Cai, C. Zhao, H. Tang and L. He, *Adv. Energy Mater.*, 2024, **14**, 2402306.

56 P. Jiang, Q. Du, C. Lei, C. Xu, T. Liu, X. He and X. Liang, *Chem. Sci.*, 2024, **15**, 3357.

57 X. Li, S. Wang, D. Zhang, P. Li, Z. Chen, A. Chen, Z. Huang, G. Liang, A. L. Rogach and C. Zhi, *Adv. Mater.*, 2023, **36**, 2304557.

58 Z. Zhang, Y. Li, F. Mo, J. Wang, W. Ling, M. Yu and Y. Huang, *Adv. Mater.*, 2024, **36**, e2311914.

59 L. Yan, L. Liu, C. Qiu, Y. Xiang, H. Yu, L. Zhang, T. F. Yi, Y. Wang and J. Shu, *Angew. Chem., Int. Ed.*, 2025, e202506466.

60 S.-J. Zhang, J. Hao, H. Wu, Q. Chen, Y. Hu, X. Zhao and S.-Z. Qiao, *J. Am. Chem. Soc.*, 2025, **147**, 16350.

61 M. Wang, Y. Meng, M. Sajid, Z. Xie, P. Tong, Z. Ma, K. Zhang, D. Shen, R. Luo, L. Song, L. Wu, X. Zheng, X. Li and W. Chen, *Angew. Chem., Int. Ed.*, 2024, e202404784.

62 W. Yan, W. Liu, J. Qiu, F. Tan, J. Liang, X. Cai, C. Dai, J. Zhao and Z. Lin, *Nat. Commun.*, 2024, **15**, 9702.